First publ. in: The EMBO Journal 22 (1999), pp. 6228-6239

Crystal structure of human β2-glycoprotein I: implications for phospholipid binding and the antiphospholipid syndrome

Robert Schwarzenbacher, Kornelius Zeth[1], Kay Diederichs[2], Anna Gries[3], Gerhard M.Kostner[4], Peter Laggner and Ruth Prassl[5]

Institute of Biophysics and X-ray Structure Research, Austrian Academy of Sciences, Steyrergasse 17/6, A-8020 Graz, [3]Institute of Physiology and [4]Institute of Medical Biochemistry, University of Graz, Harrachgasse 21, A-8010 Graz, Austria, [1]MPI for Biochemistry, Department of Molecular Structural Biology, Am Klopferspitz 18a, D-82152 Martinsried and [2]Faculty of Biology, University of Konstanz, POB-55 60, D-78457 Konstanz, Germany

[5]Corresponding author
e-mail: ruth.prassl@oeaw.ac.at

The high affinity of human plasma β2-glycoprotein I (β_2GPI), also known as apolipoprotein-H (ApoH), for negatively charged phospholipids determines its implication in a variety of physiological pathways, including blood coagulation and the immune response. β_2GPI is considered to be a cofactor for the binding of serum autoantibodies from antiphospholipid syndrome (APS) and correlated with thrombosis, lupus erythematosus and recurrent fetal loss. We solved the β_2GPI structure from a crystal form with 84% solvent and present a model containing all 326 amino acid residues and four glycans. The structure reveals four complement control protein modules and a distinctly folding fifth C-terminal domain arranged like beads on a string to form an elongated J-shaped molecule. Domain V folds into a central β-spiral of four antiparallel β-sheets with two small helices and an extended C-terminal loop region. It carries a distinct positive charge and the sequence motif CKNKEKKC close to the hydrophobic loop composed of residues LAFW (313–316), resulting in an excellent counterpart for interactions with negatively charged amphiphilic substances. The β_2GPI structure reveals potential autoantibody-binding sites and supports mutagenesis studies where Trp316 and CKNKEKKC have been found to be essential for the phospholipid-binding capacity of β_2GPI.

Keywords: apolipoprotein H (ApoH)/complement control protein/β2-glycoprotein I/short consensus repeat/sushi domain

Introduction

The immune response, complement regulation and receptor recognition mechanisms are often facilitated by specific proteins built up of a series of consecutive short consensus repeats (SCRs). One of these members represents the five-domain protein β2-glycoprotein I (β_2GPI), also designated as apolipoprotein-H (ApoH). β_2GPI is a constituent of human plasma (0.2 mg/ml), with substantial amounts of protein associated with renal tissue and lipoprotein classes, particularly chylomicrons and high-density lipoproteins (Polz and Kostner, 1979; Klaerke *et al*., 1997). β_2GPI is a single chain glycoprotein of 326 amino acid residues (M_r ~43 kDa) containing 11 disulfide bridges and four N-linked glycosylation sites (Kristensen *et al*., 1991; Steinkasserer *et al*., 1991). It comprises four SCRs from the complement control protein (CCP) module type, also known as GP-Is or sushi domains, and an additional fifth C-terminal domain. CCPs are modules of ~60 amino acid residues, with a consensus pattern of four invariant cysteines and a small number of additional conserved residues (Bork *et al*., 1996). The fifth domain consists of residues 244–326 and is stabilized by three internal disulfide bonds. It carries a lysine-rich domain and has a definite positive charge character (Sanghera *et al*., 1997). Due to that architecture, β_2GPI binds to negatively charged surfaces including heparin, DNA (Schousboe, 1988), cell membranes, endothelial cells (Delpapa *et al*., 1998), macrophages (Balasubramanian and Schroit, 1998) and acidic phospholipids. Acidic phospholipid species are normally found in the interior of cells but become exposed when cells undergo apoptosis and senescence. At this stage, the phospholipids may become the target of β_2GPI, which further induces the recognition, binding and clearance of macrophages (Balasubramanian and Schroit, 1998). Complexes formed by β_2GPI and acidic phospholipids are suggested to act as antigen for autoimmune antiphospholipid antibodies (aPLAs) associated with clinical events such as antiphospholipid syndrome (APS), lupus erythematosus, thrombosis and recurrent fetal loss (McNeil *et al*., 1990; Guerin *et al*., 1997; Gharavi *et al*., 1998). It has been proposed that domain V possesses both the phospholipid-binding site and the epitope for aPLAs (Hunt and Krilis, 1994), whereas another group reports on the involvement of CCP1 in lipid–protein interaction (Hagihara *et al*., 1995). It is not yet clear whether aPLAs recognize epitopes displayed by native β_2GPI or new epitopes expressed after binding of the molecule to negatively charged structures (Galli *et al*., 1990). Studies using aPLAs from patients with APS and domain-deleted mutants of human β_2GPI revealed that the target site of some aPLAs appears to reside in domain IV (Hasunuma *et al*., 1997; George *et al*., 1998). Here, the identification of the precise role of β_2GPI in the autoimmune response is of extreme importance and a key step towards the development of new concepts in medical APS therapy as attractive alternatives to conventional methods such as plasmapheresis.

Besides its role in the autoimmune response, β_2GPI acts as a natural anticoagulant through inhibition of the prothrombinase activity of ADP-activated platelets (Nimpf *et al*., 1986; Shi *et al*., 1993). Furthermore, β_2GPI binds

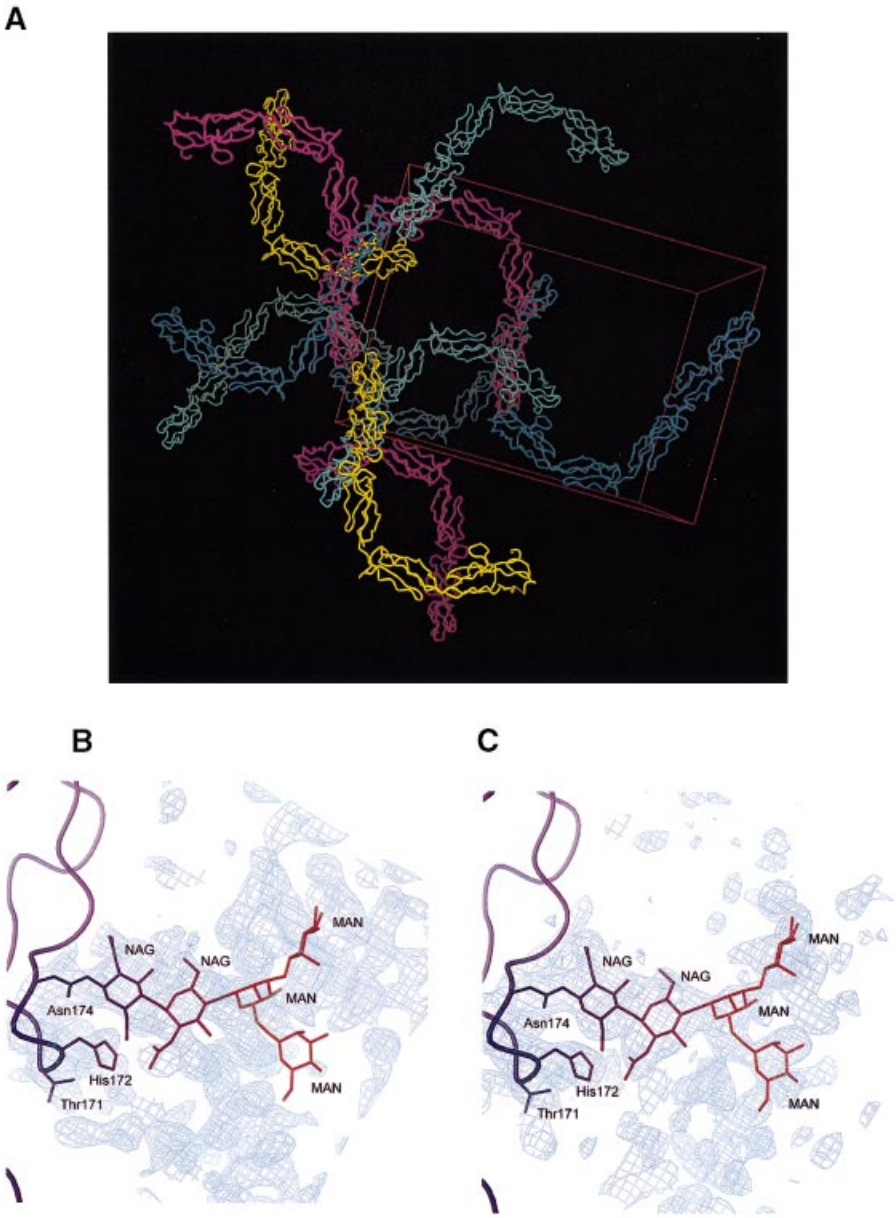

Fig. 1. (**A**) Crystal packing of β_2GPI reveals one molecule in the asymmetric unit with a remarkably high solvent content of ~84%. Individual molecules in the same orientation are shown in corresponding colours. The unit cell is indicated in red ($C222_1$, a = 159.5 Å, b = 164.8 Å, c = 114.3 Å). (B and C) Electron density maps showing the N-linked glycan residue attached to Asn174 in CCP3. Both maps are contoured at a level of 1.5σ. The refined model is shown with colour coding according to the individual *B*-factors. The colour spectrum ranges linearly from blue (5 Å^2) to red (170 Å^2). (**B**) Experimental SHARP/SOLOMON (Bailey, 1994; La Fortelle and Bricogne, 1997) map at 2.87 Å. (**C**) Final $2F_o - F_c$ map at 2.87 Å. All figures are prepared using the program DINO [DINO: Visualizing Structural Biology (1999) http://www.bioz.unibas.ch/~xray/dino] except where stated otherwise.

to oxidatively modified low-density lipoprotein (LDL), implying a direct influence on receptor-mediated endocytosis of LDL (Hasunuma *et al*., 1997; Horkko *et al*., 1997) and hence suggests a functional role for β_2GPI in the progress of atherosclerosis. Recently, new functions of β_2GPI correlated to its binding capacity have been reported, i.e. β_2GPI binds to hepatitis B virus antigen (Mehdi *et al*., 1994, 1996), exhibits receptor recognition features and binds to the renal epithelial endocytotic receptor megalin (Moestrup *et al*., 1998) where it serves as a marker for renal tubular disease (Klaerke *et al*., 1997).

CCP domains are common in many proteins (>140) involved in the complement regulatory system, such as complement factor H, CR1, C1, C2 and C4BP, and in blood coagulation, such as factor XIII (Davie *et al*., 1986), or are present in various virus-binding complement control proteins as well as cell surface proteins including interleukin-2 receptor, α-chain haptoglobin and selectins (Bork *et al*., 1996). The NMR structures of fragments of factor H (FcH) (Barlow *et al*., 1993), the C-terminal half of the vaccinia virus complement control protein (VCP) (Wiles *et al*., 1997) and, only recently, the crystal structure of the measles virus-binding region of CD46 (Casasnovas *et al*., 1999) have revealed a characteristic β-sandwich fold for the CCP module. The number of proteins that have been identified as containing CCP domains is growing

rapidly, coinciding with increasing functional activities. The crystal structure of β_2GPI is the first that provides information on the arrangement of four consecutive CCP modules in an intact protein followed by a new phospholipid-binding domain.

Results and discussion

Structure determination

β_2GPI was purified from citrated human plasma by treatment with perchloric acid followed by affinity chromatography over heparin–Sepharose (Gries *et al*., 1989). Crystals of β_2GPI were grown by vapour diffusion techniques at 277K as described previously (Saxena *et al*., 1998). Derivatives were obtained by co-crystallization with 0.5 mM $K_2PtCl_4/PtCl_4$ under identical conditions. The crystals belong to the space group $C222_1$ (a = 159.5 Å, b = 164.8 Å, c = 114.3 Å), containing only one molecule per asymmetric unit resulting in a remarkably high solvent content of ~84%. The extraordinary crystal packing is shown in Figure 1A. Native and derivative crystals diffracted under cryo-cooled conditions in a synchrotron beam to 2.6 and 3.2 Å, respectively. Phases from two Pt derivatives and from a two wavelength Pt-MAD experiment were combined to calculate a 2.87 Å SHARP/SOLOMON map (Bailey, 1994; La Fortelle and Bricogne, 1997), in which the initial model was built using program O (Jones *et al*., 1991). Subsequent cycles of rebuilding and refinement in CNSsolve (Brünger *et al*., 1998) yielded a final model containing all 326 amino acid residues, seven *N*-acetylglucosamins, four mannose and 22 ordered water molecules. As an example, the experimental and final difference maps in the section of Asn174 are shown on top of the final model in Figure 1B and C, respectively. The crystallographic *R*-factor for the present model and all available data between 50 and 2.87 Å is 23.8%. The corresponding free *R*-factor is 24.4%, calculated with 5% of the data. The model showed good geometry, with all non-glycine residues in allowed and generously allowed regions of the Ramachandran plot. The structure has low r.m.s. bond distance (0.009 Å) and bond angle (1.5°) deviations (PROCHECK, Laskowski *et al*., 1993). Relevant statistics are given in Table I.

Table I. Phasing and refinement statistics of β_2GPI

	Native	Pt-I	Pt-II	Pt-λ_1	Pt-λ_2
Data collection and phasing statistics					
Wavelength (Å)	0.95	1.06	1.07	1.0707	0.8434
Resolution (Å)	50–2.87	50–3.3	50–3.2	50–3.4	50–3.4
Reflections (observed)	103 699	77 896	82 473	82 673	82 411
Reflections (unique)	32 406	26 810	23 556	20 513	19 482
Completeness (%)	93.2 (60.1)	94.2 (94.2)	87.3 (87.0)	99.8 (98.3)	96.2 (95.4)
R_{merge}[a] (%)	8.6 (43)	10.4 (38)	13.2 (32)	9.2 (36)	9.3 (36)
I/σ (I)	13.3 (2.7)	9.7 (2.7)	10.2 (1.9)	11.4 (2.1)	11.3 (2.0)
Model refinement statistics					
Resolution range (Å)	50–2.87				
Reflections (total)	32 406				
R_{cryst}[b] (%)	23.75				
R_{free}[c] (%)	24.38				
Protein atoms	2540				
Glycans + glycan atoms	11 + 143				
Water molecules	22				
R.m.s.d. angles (°)	1.5				
R.m.s.d. bonds (Å)	0.009				

[a]$R_{merge} = \Sigma|I - <I>|/\Sigma I$, where I is the observed intensity and $<I>$ is the average intensity from multiple observations of symmetry-related reflections, the values in parentheses correspond to the highest resolution shell.
[b]$R_{cryst} = \Sigma|(F_{obs}) - (F_{calc})|/\Sigma\ (F_{obs})$.
[c]R_{free} = same as R_{cryst} but comprises a test set (5% of total reflections), which was not used in model refinement.

Fig. 2. (**A**) The secondary structural elements of β_2GPI shown as a ribbon drawing. The β-strands are shown in blue. Each CCP domain contains either six (CCP2) or seven (CCP1, CCP3 and CCP4) β-strands. The fifth module contains four β-strands, one α-helix (residues 263–266) and the short 3_{10} helix formed by residues 320–322; both helices are shown in red. Disulfide bonds are displayed in yellow. The four N-linked carbohydrates attached to residues Asn143 (NAG327, NAG328), Asn164 (NAG329), Asn174 (NAG330, NAG331, MAN332, MAN333, MAN334) and Asn234 (NAG335, NAG336, MAN337) are shown in all-atom representation. (**B**) Topological diagram of β_2GPI as derived from PROCHECK (Laskowski *et al*., 1993). The β-strands of each CCP module are coloured differently: CCP1 (yellow), CCP2 (green), CCP3 (red), CCP4 (blue) and the fifth domain is in white. The two helical segments are in grey. The main chain hydrogen bonds are indicated with dashed lines. The four glycosylation sites are marked with black spheres. The motif (KNKEKK) spanning residues 282–287 is presented. The black arrow indicates the plasmin cleavage site between residues K317 and T318. (**C**) Stereoview ribbon representation of structurally superimposed CCP modules. CCP1–CCP4 are coloured as outlined in (B). Structurally conserved residues, drawn in all-atom mode are: CCP1 (C4, P5, P7, V15, L18, P24, E26, I28, Y30, C32, Y36, F45, C47, W53, L58, C60); CCP2 (C65, P66, A68, V76, Y78, Y83, N85, I87, F89, C91, F95, L97, A103, C105, W111, P116, C118); CCP3 (C123, P124, P126, L134, Y137, Y147, D149, A151, F153, C155, Q158, H159, M161, I167, C169, W175, P179, C181, E183); and CCP4 (C186, P187, P189, V197, Y199, Y207, D209, A211, F213, C215, Y219, L221, I227, C229, W235, P239, C241). The identity of each residue is shown in one-letter code. Disulfide bridges are shown in yellow. Please note that CCP3 contains His159 instead of a tyrosine residue, Gln158 instead of a glycine residue and Glu183 instead of a proline or serine residue, conserved in the majority of CCPs. Relevant statistics are given in Table III. The alignment was performed with the program TOP (Lu, 1996).

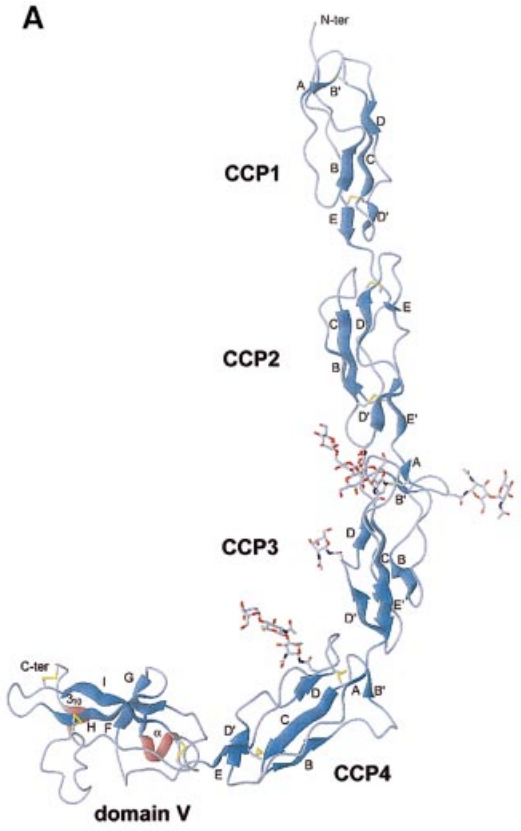
A
N-ter
CCP1
CCP2
CCP3
CCP4
C-ter
domain V

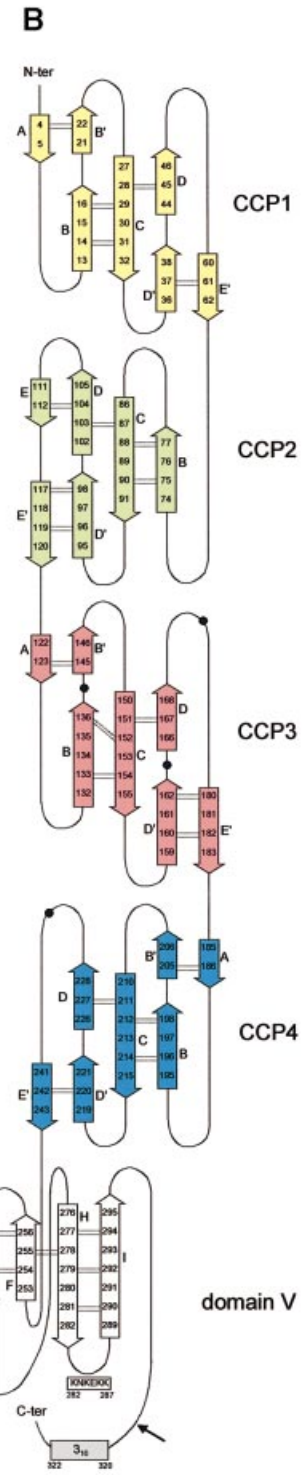
B
N-ter
CCP1
CCP2
CCP3
CCP4
domain V
C-ter

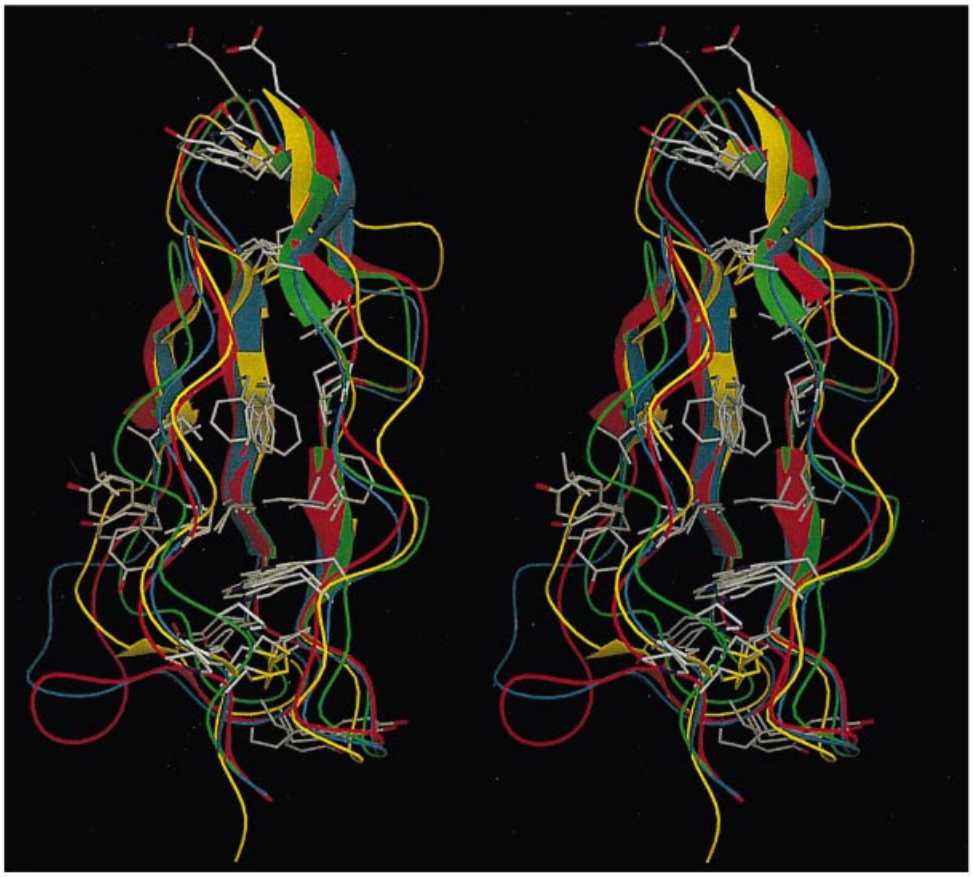
C

Overall structure of β_2GPI

The crystal structure of β_2GPI reveals five domains joined like beads on a string to form an elongated J-shaped molecule with overall dimensions of 132 × 72 × 20 Å (Figure 2). The four N-terminal CCP modules are arranged along their long axis in a slight right-handed spiral to join the distinct fifth domain. CCPs 1–4 are very similar (Figure 2C) in terms of an elliptical β-sandwich structure with overall dimensions of ~38 × 17 × 20 Å. The secondary structure of a module is comprised of several short, antiparallel β-strands wrapped around a well defined hydrophobic core. The structure is stabilized by two disulfide bonds that are N- and C-terminally disposed at opposite poles of the module. The β-strands run approximately parallel and antiparallel to the long axis, with the first and third turns located close to the C-terminus and the second and fourth turns near the N-terminus. The main antiparallel β-sheet is formed by strands B, C and D in CCP1, CCP3 and CCP4, and by strands B, C, D and E in CCP2. An additional short β-sheet composed of strands A and B′ located near the N-terminus is present in CCP1, CCP3 and CCP4. The C-terminal counterpart with strands D′ and E′ is observed in each of the four modules (Figure 2A and B). Most of the hydrophobic residues contribute to the core; exceptions are aromatic residues close in space to the termini.

The fifth domain comprises residues 244–326 and folds into a central β-spiral composed of four antiparallel β-sheets, namely F, G, H and I. It also contains one short α-helix between strands G and H and an extended loop region terminated by a short piece of 3_{10} helix close to the C-terminus. The structure is held together by three disulfide bridges in a 1–4, 2–5, 3–6 pattern (Figure 2A and B). Comparison with known protein structures (using program DALI, Holm and Sander, 1993) did not reveal any other folds that would superimpose well (score >2.6). In the crystal structure of β_2GPI, we have identified four N-linked glycosylation sites; three of the glycans are located in CCP3, the remaining one is part of CCP4. Glycosylation sites Asn143 and Asn164 show density for two and one *N*-acetylglucosamine molecule, respectively, whereas Asn174 and Asn243 allowed for the modelling of two *N*-acetylglucosamine and three and one mannose molecule, respectively. The functional role of the carbohydrate moiety is not yet clear; however, a varying degree of glycosylation *in vivo* leads to inhomogeneity of the protein and allows for the isolation of distinct isoforms.

Crystal packing

The extravagant crystal packing may suggest a rigid nature of the elongated molecule, which is in contrast to the flexibility observed in the crystal structure of CD46. Analysis of the crystal contacts (Figure 1A) shows that each molecule has five neighbours, with one major contact site extending from CCP1 to the beginning of CCP3 involving strands A, B, B′ and the C–D′ loop of CCP1, strands D, E and E′ of CCP2, as well as strand A, the D–E′ loop and the glycan chain attached to Asn174 of CCP3. The next crystal contact contains hydrophobic interactions between CCP1 and CCP1 mediated by residues 24–25 and 46–49. Further hydrophobic contacts exist between residues 69–73 of CCP2 and the C–D′ loop of CCP4 as well as residues 243–247 of domain V. The interaction between domain V and domain V contains residues 258–260 and 322–325. These contacts indicate potential sites for protein–protein interactions relevant for β_2GPI function and recognition by aPLAs.

Architecture and similarity of CCPs

The superposition of CCPs 1–4 in β_2GPI is shown in Figure 2C and the statistics are summarized in Table II. This alignment reveals extensive conservation of residues found in the core and especially in the region of the central β-sheet from strand C to strand D. Inspection of the sequence alignment of homologous proteins containing four consecutive CCP modules (Figure 3A), namely β_2GPI, VCP, CD46 and Hikaru genki protein, in the light of the β_2GPI structure highlights the presence of three regions where most of the insertions occur. There is one hypervariable loop connecting strands B and B′, which appears to be particularly prominent in CCP3 of β_2GPI and CCP1 of VCP. The next site resides between strands D′ and D. Here, CCP4 and CCP1 of β_2GPI show insertions of one and two residues at the β-bulge. The turn between strand D and the conserved tryptophan is another, albeit rare, site for insertions, which is only present in CCP2 of VCP and CD46.

In general, the secondary structural elements of the CCP modules found in the structures of β_2GPI, VCP and CD46 coincide well. Interestingly, the two CCPs from VCP reveal the 'eight β-strand' pattern, which seems typical for a CCP module, whereas the CCPs from β_2GPI and CD46 show various exceptions. In β_2GPI, we observe the following: CCP1 lacks strand E; CCP2 lacks strands A and B′; and CCP3 as well as CCP4 lack strand E. The exceptions in CD46 are: strand A and B′ in CCP1 are missing while strand E′ is more pronounced and fuses with strand A of CCP2. In addition, CCP2 shows a very prominent central β-sheet but lacks strand E′.

Modular arrangement

The relative orientation of various repeats, classically expressed in terms of tilt and twist angles (Bork *et al*., 1996), represents an important parameter for the overall architecture of SCRs. As seen in Table III, these angles vary drastically within the molecule, showing small tilts between CCP1 and CCP2, and between CCP2 and CCP3. This is in contrast to the strong bent observed between CCP3 and CCP4, between CCP4 and domain V, and in the other structures reported that have pairs of CCP domains such as CD46, VCP and FcH. In all these cases, tilt angles of ~60° have been observed.

For comparison, residues located at the intermodular interface from β_2GPI, CD46 and VCP are highlighted in Figure 3A. The interdomain linker that is bordered by the two disulfide bonds spans only four amino acid residues and contributes a critical part to the spatial conformation of the molecule. A typical CCP intermodular linker is composed of residues that are either hydrophobic (APVIL) or, if charged, contain alkyl chains with more than two methylene groups (KRE). These residues are long enough for the hydrophobic part of the side chain to pack against the core, leaving the charged portion solvent exposed. Exceptions in β_2GPI are Thr61 located at the surface and the buried Ser244, which is involved in a hydrogen-bonding network. Common to the CCPs in β_2GPI and

Table II. Topological comparison of the CCP modules in β_2GPI, CD46, VCP and FcH

		β_2GPI CCP1	β_2GPI CCP2	β_2GPI CCP3	β_2GPI CCP4
β_2GPI	CCP2	1.82 (15) [43]	–	–	–
	CCP3	1.49 (10) [50]	1.49 (16) [50]	–	–
	CCP4	1.54 (10) [42]	1.74 (2) [23]	1.20 (19) [55]	–
CD46	CCP1	1.45 (15) [46]	1.48 (4) [23]	1.42 (6) [43]	1.54 (4) [39]
	CCP2	2.24 (4) [25]	1.22 (0) [13]	1.76 (10) [45]	1.38 (0) [6]
VCP	CCP3	1.39 (8) [24]	1.85 (8) [32]	1.53 (7) [41]	1.71 (2) [20]
	CCP4	1.93 (12) [44]	1.44 (17) [44]	1.61 (1) [20]	1.18 (16) [43]
FcH	CCP15	2.09 (11) [43]	1.28 (8) [29]	1.92 (9) [49]	1.65 (6) [28]
	CCP16	1.70 (11) [29]	NFA[a]	1.65 (6) [46]	NFA

[a]No feasible alignment.
For each comparison, the first number indicates the r.m.s.d (Å) between equivalent C_α residues. The middle (in parentheses) and last (in brackets) numbers indicate the number of identical and matching residues, respectively, as calculated with the program TOP (Lu, 1996).

VCP, and to CCP1 of CD46, is the fact that strand E′ continues beyond the last cysteine and stabilizes the first N-terminal part of the linker region. The second part of the CCP module linker is usually stabilized by strand A, with exceptions in CCP2 and CCP3 of β_2GPI.

In addition to the linker region, there are two sites in each of the neighbouring modules contributing to the interface. The interactions are characterized mainly by the residues located in the first and third turns of the N-terminal module as well as in the second and fourth turns of the C-terminal module. The major site of interaction in the N-terminal module comes from 4–6 mostly hydrophobic residues located at strand D′, whereas the two residues at the beginning of strand B add only minor interactions. Interestingly, the C-terminal module, with two regions of ~3–9 and 4–7 residues, contributes a predominantly larger number of side chains to the interface. These residues are located in the region of strand B′ or the B–C loop and also in the D–E or D–E′ loop. Analysis of the interacting residues in the CCP interfaces of β_2GPI reveals that residues at strand D′ from the N-terminal module are interacting mainly with the D–E′ loop but also to a varying degree with the B–C loop of the C-terminal module. Remarkably, all tilt angles observed to date are between 0° and 60°, whereas the observed twist angles show no definite range. For comparison, a superposition of pairs of CCPs with a tilt angle of ~60° is given in Figure 3B. The intermodular interfaces found in β_2GPI, CD46, FcH and VCP show that despite the similarity of CCP modules, there is no obvious correlation to the modular orientation in terms of twist angles.

CCP1 and the CCP1–2 interface

The main chain of CCP1 shows the lowest r.m.s.d. with CCP3 in VCP, whereas the highest number of matching residues is shared with CCP3 of β_2GPI (Table II). The backbone differs from the other CCPs in β_2GPI at residues 38–43 (D′–D loop) and residues 54–58 (D–E loop) (Figure 3A and C). CCP1 has no distinct charge character despite a positively charged patch made up by residues Arg34, Arg39 and Lys52 (Figure 4). It may be noted that the suggestion of a calmodulin-binding site requiring the formation of a basic amphiphatic helix between residues 32 and 47 (Rojkjaer *et al*., 1997) is, at least from a structural point of view, very unlikely. As most of the residues are involved in β-strands (32 in C, 36–38 in D′ and 44–46 in D), they provide an unfavourable starting point for such a huge conformational change to occur. Furthermore, the blueshift of intrinsic tryptophan fluorescence from 352 to 342 nm as reported by the same group (Rojkjaer *et al*., 1997) does not correspond to a deeply buried tryptophan as present in CCP1. Hence, this observation is more likely to be explained by Trp316 suggesting a putative calmodulin-binding site in domain V.

In showing no tilt angle, with a twist angle of ~115° the CCP1–2 interface is an exception among the CCP module pairs studied to date. The buried area at the interface is 320 Å^2 (Table III). Main chain hydrogen bonds are formed between Thr61(O) and Val37(N), Gly35(O) and Arg63(N), Arg63(O) and Tyr83(N), and Phe81(O) and Cys65(N). The remaining interactions at the interface involve hydrophobic contacts between Phe12, Tyr36, Val37, Gly35, Tyr83, Pro84, Pro62 and the backbone of Arg63 (Figure 5A).

CCP2 and the CCP2–3 interface

CCP2 shows the lowest r.m.s.d. of equivalent C_α atoms with CCP2 of CD46, whereas the highest number of matching residues is shared with CCP3 of β_2GPI (Table II). CCP2 lacks strands A and B′ and has no distinct charge character (Figures 3A and 4). The CCP2–3 interface shows a low tilt angle of ~30° and is unusual in having a remarkably low buried interface surface area of 207 Å^2 (Table III). Main chain hydrogen bonds are formed between Ala119(O) and Tyr96(N), Gly94(O) and Ile121(N), and Ser140(O) and Cys123(N). Residues Ile121, Ile122, Gly94, Phe95, Tyr96, Pro120, Ile122, Ala141, Leu146, Tyr147 and Thr171 stabilize the interface by van der Waals interactions and contribute, together with three ordered water molecules, to the solvent-inaccessible shell of the CCP2–3 interface (Figure 5B).

CCP3 and the CCP3–4 interface

CCP3 contains three N-glycosylation sites and is therefore the most highly glycosylated CCP module described to date. It reveals the lowest r.m.s.d. of equivalent C_α atoms and the highest number of matching residues with CCP4 of β_2GPI (Table II). The largest deviation from the common CCP fold is an insertion between strands B and B′ comprising residues 138–145 (Figure 2C). This insertion makes an extra turn and includes the glycosylated Asn143 with the 1-N-linked NAG327 and the 1–4-linked NAG328. Further N-glycosylation sites are Asn164 with the 1-N-linked

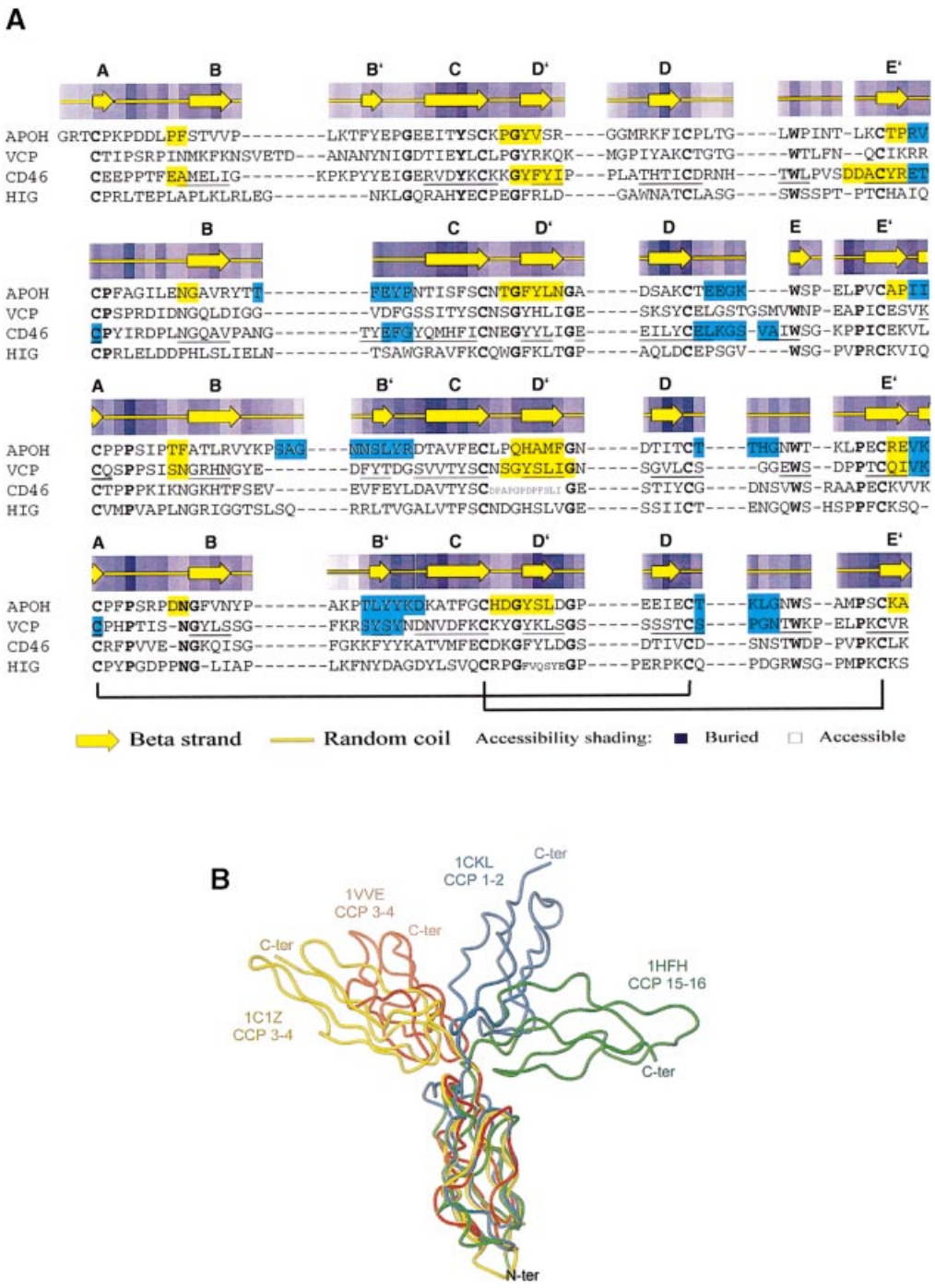

Fig. 3. (**A**) Sequence alignment of homologous proteins containing four consecutive CCP modules. ApoH (β2-glycoprotein-I; P02749) VCP (vaccinia virus 35 kDa protein; P10998); CD46 (measles virus-binding protein; P15529) and HIG (Hikaru genki, Q09109; a protein from *Drosophila* that belongs to both the immunoglobulin and complement-binding protein superfamilies). Highly conserved amino acid residues are highlighted in bold. The secondary structural elements and accessibilities as derived from the crystal structure of β_2GPI are indicated above the sequence of ApoH. The identity of each residue is shown in one-letter code. For comparison, residues forming β-strands in the reported structures of CD46 (CCP1–CCP2) (Casasnovas *et al*., 1999) and VCP (CCP3–CCP4) (Wiles *et al*., 1997) are underlined. The amino acid residues contributing to the module interface are highlighted in yellow (residues from the N-terminal module) and turquoise (residues from the C-terminal module). The disulfide bonding pattern is indicated with black lines at the bottom. (**B**) Orientational differences in fragments with two CCPs showing high tilt angles (~60°). Superimposed structures of: β_2GPI, 1C1Z CCP3–CCP4 (yellow); VCP, 1VVE CCP3–CCP4 (red) (Wiles *et al*., 1997); CD46, 1CKL CCP1–CCP2 (blue) (Casasnovas *et al*., 1999); and FcH, 1HFH CCP15–CCP16 (green) (Barlow *et al*., 1993). The structures were superimposed with respect to their N-terminal CCP using TOP (Lu, 1996).

NAG329 and Asn174 with the 1-N-linked NAG330, the 1–4-linked NAG331, the 1–4-linked MAN332, the 1–3-linked MAN333 and the 1–6-linked MAN334.

Note that CCP3 contains three critical differences from the consensus sequence: His159 replaces the tyrosine residue; Gln158 replaces the glycine residue; and Glu183 replaces the proline or serine residue (Figure 2C). This exchange for charged and bulky side chains that are

Table III. Molecular architecture of β_2GPI

	Tilt (°)	Twist (°)	Buried area (Å^2)	Linker
CCP1–CCP2	~0	~115	320	TPRV
CCP2–CCP3	~30	~110	207	APII
CCP3–CCP4	~55	~40	335	REVK
CCP4–domain V	~55	~ −50	318	KAS

Tilt and twist angles are defined as described by Bork *et al*. (1996). The angles are calculated based on the conserved Trp residues, which are used to define the repeat axes (Bork *et al*., 1996) (except for CCP4–domain V). The program GRASP (Nicholls *et al*., 1991) was used to calculate the buried surface area for one accessible molecular surface per module.

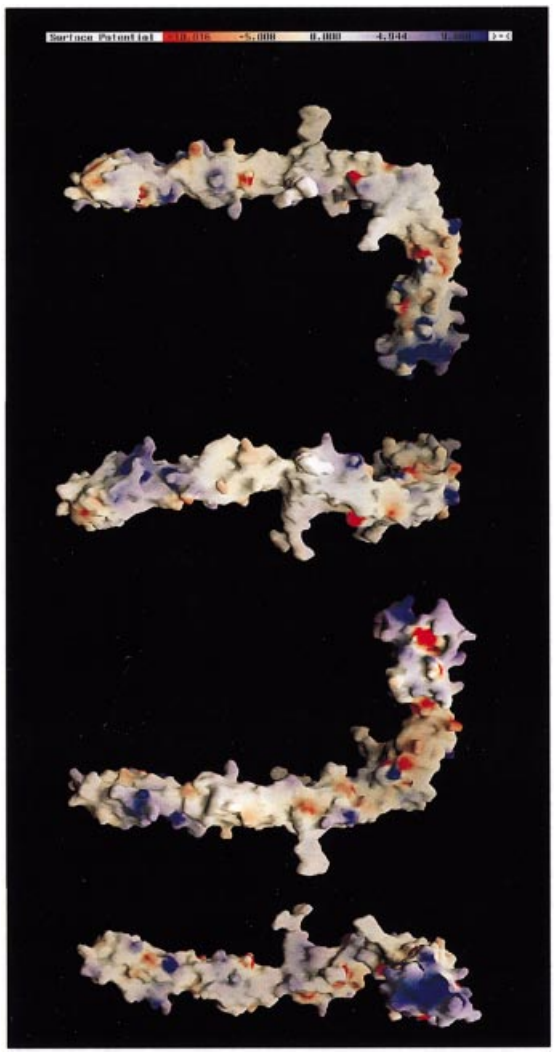

Fig. 4. GRASP molecular surface representation of β_2GPI. The four panels show the molecular surface coloured according to the electrostatic potential (red = negative, blue = positive, white = uncharged), with descending frames corresponding to successive 90° rotations about a horizontal axis. The figure was generated using the program GRASP (Nicholls *et al*., 1991).

directly located at the interface agrees with the observed tilt angle of ~55°. In addition, the interface accommodates Tyr206 from CCP4 and shows the largest buried surface area (335 Å^2) as well as the lowest twist angle (~40°) found in β_2GPI (Table III). Main chain hydrogen bonds are formed between Ala160(O) and Arg182(N), and Arg182(O) and Ala160(N). Hydrophobic interactions exist between Phe131, Ala160, Phe162, Val184, Tyr207 and the backbone of side chains Arg182, Glu183, Gln158, Tyr206, Lys185 and Lys231 (Figure 5C).

CCP4 and the CCP4–domain V interface

CCP4 reveals the lowest r.m.s.d. of equivalent C_α atoms and the highest number of matching residues with CCP4 of VCP (Table II). CCP4 has no distinct charge character (Figure 4) and contains an insertion between strands B and B′ comprising residues 201–205 (Figure 2C). The most striking feature is Tyr206 next to the highly conserved Tyr207, which protrudes into the CCP3–4 linker domain. CCP4 contains one glycosylation site at Asn234 with the 1-N-linked NAG335, the 1–4-linked NAG336 and the 1–4-linked MAN337. The linker contains only three residues (KAS) with a tilt angle of ~55° and a negative twist angle (approximately –50°) and a buried interdomain area of 318 Å^2. Main chain hydrogen bonds are formed between Ser220(O) and Lys242(N), Lys242(O) and Ser220(N), Ala243(O) and Asp298(N), and Asp298 (OD) and Ala243(N). Additional stabilization comes from three ordered water molecules that are involved in a tight hydrogen-bonding network through residues Asp217(O)–HOH352–Ser244(OG), Ser220(OG)–HOH345–Ser244(OG), HOH345–Lys242(O) and HOH357–Ser244(O). van der Waals interactions are formed between Asn194, Tyr219, Ala243 and the backbones of Lys242 and His273 (Figure 5D).

Domain V and implications for lipid binding

Domain V is characterized by an unusual amino acid composition. The sequence is rich in lysine residues (18%) and contains the remarkable sequence motif CKNKEKKC (281–288). Electrostatic calculations show that the fifth domain has an overall positive charge character most pronounced at the C-terminal pole region in close proximity to the hydrophobic loop composed of residues LAFW (313–316) (Figure 6A, B and C). It is noteworthy that this loop, despite its apolar nature, is surface exposed but not involved in any crystal contacts. Furthermore, these residues, especially Phe315, show high temperature factors, indicating potential flexibility (Figure 6A). Consequently, this domain provides an excellent counterpart for electrostatic interactions with negatively charged amphiphilic substances. Thus, the present structure supports mutagenesis studies where Trp316, the CKNKEKKC motif and the integrity of the disulfide bonds have been found to be essential for the lipid-binding capacity of β_2GPI (Hunt and Krilis, 1994; Sanghera *et al*., 1997; Horbach *et al*., 1998). A genetically determined single mutation that results in the amino acid substitution of Trp316 by Ser316 completely abolishes the phospholipid-binding capacity of β_2GPI (Sanghera *et al*., 1997; Horbach *et al*., 1998), which serves as strong biochemical evidence for the involvement of the surface-located Trp316 in the binding processes. This finding is also consistent with the fact that a nicked form of β_2GPI, produced by plasmin and factor Xa, through cleaving at residues Lys317–Thr318, lacks the ability to interact with cardiolipin (Ohkura *et al*., 1998). Cleavage at this site obviously disrupts the integrity of the LAFW (313–316) motif, as it is already located in a loop region with very high temperature

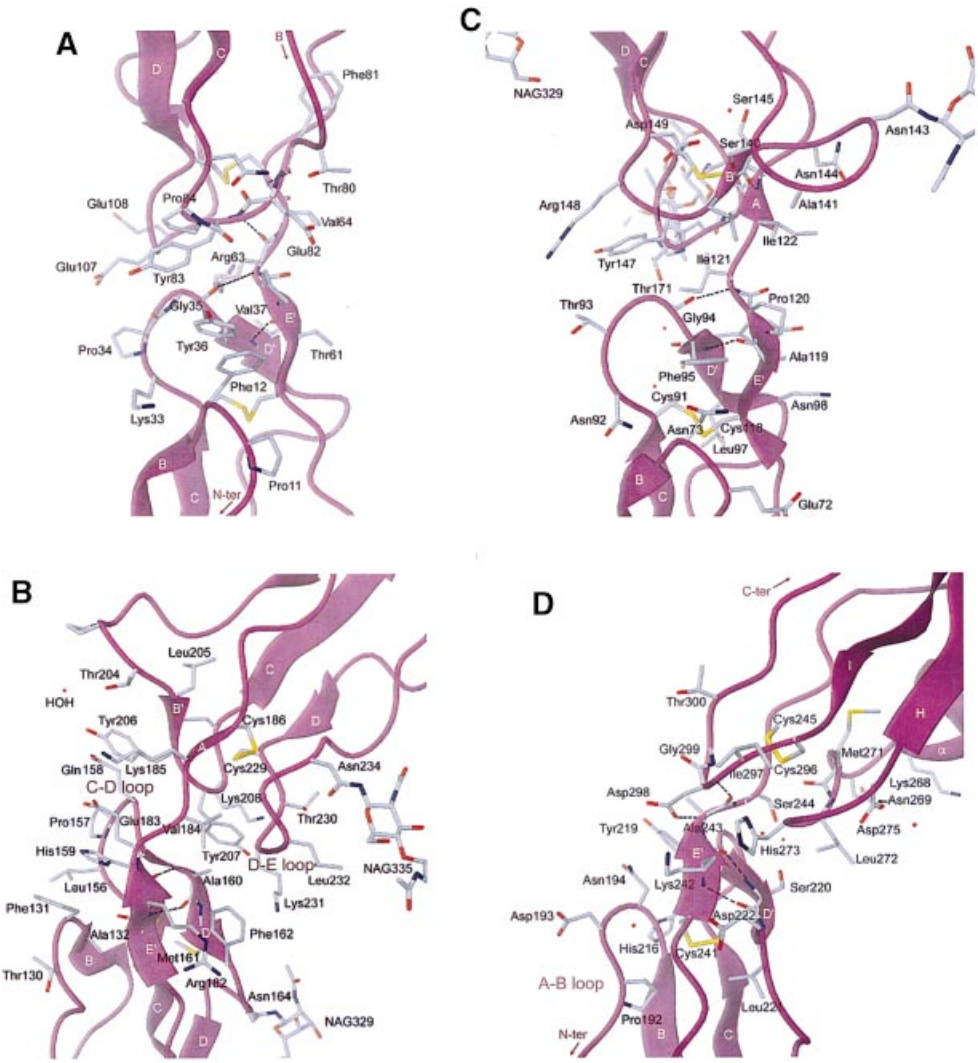

Fig. 5. Close up view of the four β_2GPI interdomain interfaces between (A) CCP1 and CCP2, (B) CCP2 and CCP3, (C) CCP3 and CCP4 and (D) CCP4 and domain V. The backbone is shown in ribbon representation with the residues and main chain atoms relevant for the interface drawn in all-atom mode. Disulfide bonds are shown in yellow and main chain hydrogen bonds are indicated with dashed lines in black. (**A**) Main chain hydrogen bonds are formed at Thr61(O)–Val37(N), Gly35(O)–Arg63(N), Arg63(O)–Tyr83(N) and Phe81(O)–Cys65(N). The remaining interactions at the interface involve hydrophobic contacts: Phe12–Tyr36–Gly35–Tyr83–Pro84–Arg63. (**B**) Main chain hydrogen bonds are formed at Ala119(O)–Tyr96(N), Gly94(O)–Ile121(N) and Ser140(O)–Cys123(N). The hydrophobic residues Ile21, Gly94, Phe95, Pro120, Ile122, Ala141, Leu146 and Tyr147 and three ordered water molecules contribute to the solvent-inaccessible shell and stabilize the interface. (**C**) Main chain hydrogen bonds are formed at Ala160(O)–Arg182(N) and Arg182(O)–Ala160(N). Hydrophobic interactions exist at Ala160–Phe162–Val184–Tyr207 and the backbone of side chains Glu183–Glu158–Tyr206–Lys185. (**D**) Main chain hydrogen bonds are formed at Ser220(O)–Lys242(N), Lys242(O)–Ser220(N), Asp217(O)–HOH352–Ser244(OG), Ser220(OG)–HOH345–Ser244(OG), HOH345–Lys242(O), HOH357–Ser244(O), Ala243(O)–Asp298(N) and Asp298(OD)–Ala243(N).

factors. The same applies to disrupting any of the disulfide bridges between cysteines 281–306 and 288–326. Moreover, these residues remain conserved among all other known mammalian sequences of β_2GPI, i.e. bovine, dog, mouse and rat, representing 90–85% homology. To comment on Lauer *et al*. (1993) who suggests the importance of His273 for β_2GPI–cardiolipin autoantibody complex formation, we would like to note that His273 is located at the CCP4–domain V interface and is therefore not easily accessible (Figure 5D).

Conclusion

Our crystallographic study reports for the first time on the arrangement of four CCPs accompanied by a fifth domain that defines a novel type of phospholipid-binding protein. It provides a unique structural insight into the architecture of CCP modules as well as their modular arrangement and their interfaces. The β_2GPI structure questions to what extent the relative orientation of the CCP modules is dependent on intra- or intermolecular interactions. The use of several concatenated domains with expansive epitopes for a great variety of interactions has been correlated with several members of the CCP protein family (Barlow *et al*., 1993; Wiles *et al*., 1997; Casasnovas *et al*., 1999), but little is known about the function of the four CCPs in β_2GPI. Potential protein–protein interaction sites relevant for β_2GPI function and the recognition by aPLAs are indicated by the crystal structure in CCP1 and CCP2 as well as the CCP4–domain V interface. In all probability, CCPs play a critical role in orienting and docking at target surfaces preceding the binding of ligands such as acidic phospholipids and negatively charged substrates. Here,

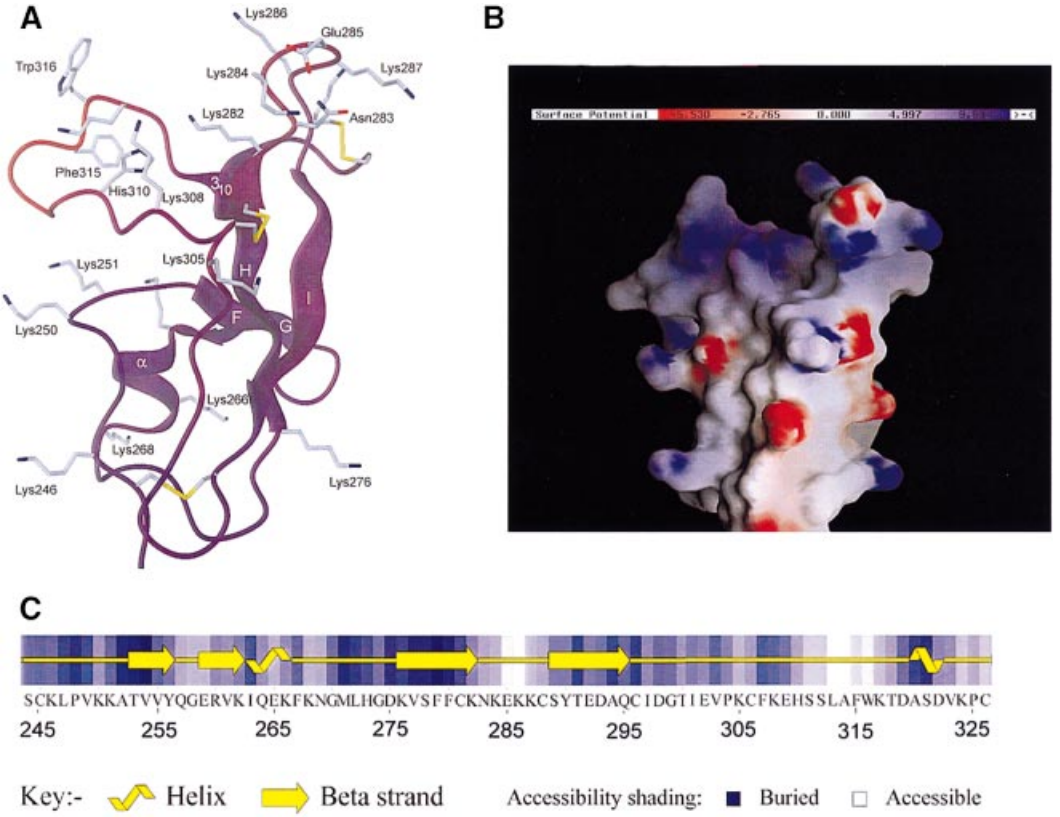

Fig. 6. (**A**) Ribbon representation of the fifth domain. The backbone is shown in colour coding according to individual *B*-factors. The colour spectrum ranges linearly from blue (5 Å^2) to red (170 Å^2). All lysines, the three disulfide bridges, the KNKEKK motif and residues His310, Phe315 and Trp316 are represented in all-atom mode. (**B**) GRASP molecular surface representation of the fifth domain of β_2GPI as shown in (A). Colour coding is according to the electrostatic potential (red = negative, blue = positive, white = uncharged). (**C**) Amino acid sequence of the fifth domain of β_2GPI (ApoH; β2-glycoprotein-I; P02749; residues 244–326). The secondary structural elements and solvent accessibilities as derived by PROCHECK (Laskowski *et al*., 1993) from the crystal structure of β_2GPI are indicated above the sequence. The identity of each residue is shown in one-letter code.

the modular architecture may provide the critical flexibility required for the recognition of the variable epitopes expressed on surfaces of lipoproteins and the extracellular matrix. The ability of β_2GPI to bind to acidic phospholipids via domain V is supported by this structural insight. Whether phospholipid binding induces some conformational changes in the β_2GPI structure as suggested by different groups (Galli *et al*., 1990; McNeil *et al*., 1990; Borchman *et al*., 1995) and whether this is critical for the recognition of the β_2GPI–phospholipid complex by aPLAs has to be clarified and awaits the results of further biochemical and structural studies. The crystallographic data presented here constitute a solid foundation for the identification of the cellular function of β_2GPI and its role in the autoimmune response, which is of extreme importance for the development of new concepts in medical APS therapy.

Materials and methods

Purification and crystallization

β_2GPI was purified from citrated human plasma by treatment with perchloric acid followed by affinity chromatography over heparin–Sepharose as described previously (Gries *et al*., 1989). Crystals of β_2GPI were grown by vapour diffusion techniques at 277K (Saxena *et al*., 1998). Typically, 3–7 mg/ml protein solution was mixed in a 1:1 ratio with reservoir solution containing 1.8 M ammonium sulfate in 10 mM Na-K-phosphate buffer pH 7.2. Crystals were obtained within 1–5 days. Derivatives were grown by co-crystallization with 0.5 mM $K_2PtCl_4/PtCl_4$ under identical conditions. Typical crystal dimensions are $0.5 \times 0.5 \times 0.8$ mm^3. Before cryo-cooling, the crystals were soaked in a cryoprotectant containing mother liquor plus 25% glycerol.

Structure determination

The crystals belong to the orthorhombic space group $C222_1$, with one molecule per asymmetric unit and an extremely high solvent content of ~84%. The unit cell dimensions are a = 159.5 Å, b = 164.8 Å, c = 114.3 Å. Native crystals diffracted up to 2.6 Å resolution and derivatives to 3.2 Å in a synchrotron beam. The native and Pt derivative data sets were collected with synchrotron radiation at the X-ray diffraction beamline XRD (ELETTRA, Trieste) using the MAR 345 scanner, while the MAD data set was collected at EMBL beamline X31 at Hasylab (DESY, Hamburg). The Pt absorption edge was determined by a fluorescence scan, and two wavelengths were selected for data collection corresponding to the maximum f'' (λ = 1.0707 Å) and the high energy remote (λ = 0.8434 Å). The data were processed using the programs DENZO (Otwinowski and Minor, 1997) and XDS (Kabsch, 1988). The Pt derivative was identified using SOLVE (Terwilliger and Berendzen, 1999). The crystal structure was solved using phases derived from two Pt derivatives and from a two-wavelength Pt-MAD experiment, which were combined to calculate a 2.87 Å SHARP/SOLOMON map (Bailey, 1994; La Fortelle and Bricogne, 1997). The initial polyalanine model (R_{free} = 46%) was built using program O (Jones *et al*., 1991) and contained a total of 260 residues, which were phased successfully using the anomalous scattering from one major and one minor platinum site. The refinement was carried out with CNSsolve (Brünger *et al*., 1998). Bulk solvent correction, simulated annealing with torsion-angle dynamics, overall anisotropic *B*-factor correction and individual *B*-factor refinement were applied. Subsequent cycles of rebuilding and refinement yielded a final model with *R*-factor = 23.8% and R_{free} = 24.4% (for all data in the region from 50 to 2.87 Å), which contained all 326 amino acid residues, seven N-acetylglucosamine, four mannose and 22 ordered

water molecules. It showed good geometry, with all non-glycine residues in allowed and generously allowed regions of the Ramachandran plot. The structure has low r.m.s. bond distance (0.009 Å) and bond angle (1.5°) deviations (PROCHECK, Laskowski *et al*., 1993). Relevant statistics are given in Table I. Accessible surface areas were calculated with GRASP (Nicholls *et al*., 1991). The quoted numbers represent the total area buried for one interacting partner. Atomic coordinates for the two-domain fragments of FcH (Barlow *et al*., 1993), the C-terminal half of VCP (Wiles *et al*., 1997) and the measles virus-binding region of CD46 (Casasnovas *et al*., 1999) were obtained from the RCSB (accession Nos 1HFH, 1VVE and 1CKL). Figures were generated with the programs DINO [DINO: Visualizing Structural Biology (1999) http://www.bioz.unibas.ch/~xray/dino] and GRASP (Nicholls *et al*., 1991).

Atomic coordinates for β_2GPI have been deposited with the RCSB, accession No. 1C1Z, and are also available from the authors.

Acknowledgements

We acknowledge the support under the TMR/LSF programme to the EMBL Hamburg Outstation, reference number: ERBFMGECT980134. This work was supported by a grant from the Fonds zur Förderung der wissenschaftlichen Forschung to R.P. (Project P11697-MED).

This article is dedicated to Professor Hans Tuppy on the occasion of his 75th birthday.

References

Bailey,S. (1994) The CCP4 suite—programs for protein crystallography. *Acta Crystallogr. D*, **50**, 760–763.

Balasubramanian,K. and Schroit,A.J. (1998) Characterization of phosphatidylserine-dependent β(2)-glycoprotein I macrophage interactions–implications for apoptotic cell clearance by phagocytes. *J. Biol. Chem.*, **273**, 29272–29277.

Barlow,P.N., Steinkasserer,A., Norman,D.G., Kieffer,B., Wiles,A.P., Sim,R.B. and Campbell,I.D. (1993) Solution structure of a pair of complement modules by nuclear magnetic resonance. *J. Mol. Biol.*, **232**, 268–284.

Borchman,D., Harris,E.N., Pierangeli,S.S. and Lamba,O.P. (1995) Interactions and molecular structure of cardiolipin and β2-glycoprotein 1 (β_2-GP1). *Clin. Exp. Immunol.*, **102**, 373–378.

Bork,P., Downing,A.K., Kieffer,B. and Campbell,I.D. (1996) Structure and distribution of modules in extracellular proteins. *Q. Rev. Biophys.*, **29**, 119–167.

Brünger,A.T. *et al*. (1998) Crystallography and NMR system: a new software suite for macromolecular structure determination. *Acta Crystallogr. D*, **54**, 905–921.

Casasnovas,J.M., Larvie,M. and Stehle,T. (1999) Crystal structure of two CD46 domains reveals an extended measles virus-binding surface. *EMBO J.*, **18**, 2911–2922.

Davie,E.W., Ichinose,A. and Leytus,S.P. (1986) Structural features of the proteins participating in blood coagulation and fibrinolysis. *Cold Spring Harb. Symp. Quant. Biol.*, **51**, 509–514.

Delpapa,N. *et al*. (1998) Human β2-glycoprotein I binds to endothelial cells through a cluster of lysine residues that are critical for anionic phospholipid binding and offers epitopes for anti-β2-glycoprotein I antibodies. *J. Immunol.*, **160**, 5572–5578.

Galli,M., Comfurius,P., Maassen,C., Hemker,H.C., de Baets,M.H., van Breda-Vriesman,P.J., Barbui,T., Zwaal,R.F. and Bevers,E.M. (1990) Anticardiolipin antibodies (ACA) directed not to cardiolipin but to a plasma protein cofactor. *Lancet*, **335**, 1544–1547.

George,J., Gilburd,B., Hojnik,M., Levy,Y., Langevitz,P., Matsuura,E., Koike,T. and Shoenfeld,Y. (1998) Target recognition of β(2)-glycoprotein I (β(2)GPI)-dependent anticardiolipin antibodies: evidence for involvement of the fourth domain of β(2)GPI in antibody binding. *J. Immunol.*, **160**, 3917–3923.

Gharavi,A.E., Cucurull,E., Tang,H., Silver,R.M. and Branch,D.W. (1998) Effect of antiphospholipid antibodies on β(2)glycoprotein I–phospholipid interaction. *Am. J. Reprod. Immunol.*, **39**, 310–315.

Gries,A., Nimpf,J., Wurm,H., Kostner,G.M. and Kenner,T. (1989) Characterization of isoelectric subspecies of asialo-β2-glycoprotein I. *Biochem. J.*, **260**, 531–534.

Guerin,J., Feighery,C., Sim,R.B. and Jackson,J. (1997) Antibodies to β(2)-glycoprotein I–a specific marker for the antiphospholipid syndrome. *Clin. Exp. Immunol.*, **109**, 304–309.

Hagihara,Y., Goto,Y., Kato,H. and Yoshimura,T. (1995) Structure and function of β2-glycoprotein I: with special reference to the interaction with phospholipid. *Lupus*, **4**, S3–S5.

Hasunuma,Y., Matsuura,E., Makita,Z., Katahira,T., Nishi,S. and Koike,T. (1997) Involvement of β(2)-glycoprotein-I and anticardiolipin antibodies in oxidatively modified low-density-lipoprotein uptake by macrophages. *Clin. Exp. Immunol.*, **107**, 569–573.

Holm,L. and Sander,C. (1993) Protein structure comparison by alignment of distance matrices. *J. Mol. Biol.*, **233**, 123–138.

Horbach,D.A., Vanoort,E., Tempelman,M.J., Derksen,R.H.W.M. and Degroot,P.G. (1998) The prevalence of a non-phospholipid-binding form of β(2)-glycoprotein I in human plasma. *Thromb. Haemost.*, **80**, 791–797.

Horkko,S., Miller,E., Branch,D.W., Palinski,W. and Witztum,J.L. (1997) The epitopes for some antiphospholipid antibodies are adducts of oxidized phospholipid and β(2) glycoprotein-1 (and other proteins). *Proc. Natl Acad. Sci. USA*, **94**, 10356–10361.

Hunt,J. and Krilis,S. (1994) The 5th domain of β(2)-glycoprotein-I contains a phospholipid-binding site (Cys281–Cys288) and a region recognized by anticardiolipin antibodies. *J. Immunol.*, **152**, 653–659.

Jones,T.A., Zou,J.Y., Cowan,S.W. and Kjeldgaard,M. (1991) Improved methods for building protein models in electron density maps and the location of errors in these models. *Acta Crystallogr. A*, **47**, 110–119.

Kabsch,W. (1988) Evaluation of single crystal X-ray diffraction data from a position sensitive detector. *J. Appl. Crystallogr.*, **21**, 916–924.

Klaerke,D.A., Rojkjaer,R., Christensen,L. and Schousboe,I. (1997) Identification of β(2)-glycoprotein I as a membrane-associated protein in kidney: purification by calmodulin affinity chromatography. *Biochim. Biophys. Acta*, **1339**, 203–216.

Kristensen,T., Schousboe,I., Boel,E., Mulvihill,E.M., Hansen,R.R., Moller,K.B., Moller,N.P.H. and Sottrup-Jensen,L. (1991) Molecular-cloning and mammalian expression of human β-2- glycoprotein-I cDNA. *FEBS Lett.*, **289**, 183–186.

La Fortelle,E.D. and Bricogne,G. (1997) Maximum-likelihood heavy-atom parameter refinement in the MIR and MAD methods. *Methods Enzymol.*, **276**, 472–494.

Laskowski,R.A., MacArthur,M.W., Moss,D.S. and Thornton,J.M. (1993) PROCHECK: a program to check the stereochemical quality of protein structures. *J. Appl. Crystallogr.*, **26**, 283–291.

Lauer,S.A., Hempel,U., Gries,A. and Frank,K.H. (1993) Amino acid sequence of the region of β2-glycoprotein 1 (gp1) which mediates binding of autoantibodies to the cardiolipin–gp1 complex in humans. *Immunology*, **80**, 22–28.

Lu,G. (1996) A WWW service system for automatic comparison of protein structures. *Protein Data Bank Q. Newsl.*, **78**, 10–11.

McNeil,H.P., Simpson,R.J., Chesterman,C.N. and Krilis,S.A. (1990) Anti-phospholipid antibodies are directed against a complex antigen that includes a lipid-binding inhibitor of coagulation: β2-glycoprotein I (apolipoprotein H). *Proc. Natl Acad. Sci. USA*, **87**, 4120–4124.

Mehdi,H., Kaplan,M.J., Anlar,F.Y., Yang,X., Bayer,R., Sutherland,K. and Peeples,M.E. (1994) Hepatitis B virus surface antigen binds to apolipoprotein H. *J. Virol.*, **68**, 2415–2424.

Mehdi,H., Yang,X. and Peeples,M.E. (1996) An altered form of apolipoprotein H binds hepatitis B virus surface antigen most efficiently. *Virology*, **217**, 58–66.

Moestrup,S.K., Schousboe,I., Jacobsen,C., Leheste,J.R., Christensen,E.I. and Willnow,T.E. (1998) β(2)-glycoprotein-1 (apolipoprotein H) and β(2)-glycoprotein-1–phospholipid complex harbor a recognition site for the endocytic receptor megalin. *J. Clin. Invest.*, **102**, 902–909.

Nicholls,A., Sharp,K.A. and Honig,B. (1991) Protein folding and association: insights from the interfacial and thermodynamic properties of hydrocarbons. *Proteins*, **11**, 281–296.

Nimpf,J., Bevers,E.M., Bomans,P.H., Till,U., Wurm,H., Kostner,G.M. and Zwaal,R.F. (1986) Prothrombinase activity of human platelets is inhibited by β2-glycoprotein-I. *Biochim. Biophys. Acta*, **884**, 142–149.

Ohkura,N., Hagihara,Y., Yoshimura,T., Goto,Y. and Kato,H. (1998) Plasmin can reduce the function of human β(2) glycoprotein I by cleaving domain V into a nicked form. *Blood*, **91**, 4173–4179.

Otwinowski,Z. and Minor,W.Z. (1997) Processing of X-ray diffraction data collected in oscillation mode. *Methods Enzymol.*, **276**, 307–326.

Polz,E. and Kostner,G.M. (1979) The binding of β2-glycoprotein-I to human serum lipoproteins: distribution among density fractions. *FEBS Lett.*, **102**, 183–186.

Rojkjaer,R., Klaerke,D.A. and Schousboe,I. (1997) Characterization of the interaction between β(2)-glycoprotein I and calmodulin and identification of a binding sequence in β(2)-glycoprotein I. *Biochim. Biophys. Acta*, **1339**, 217–225.

Sanghera,D.K., Wagenknecht,D.R., McIntyre,J.A. and Kamboh,M.I. (1997) Identification of structural mutations in the 5th domain of apolipoprotein H (β2-glycoprotein-I) which affect phospholipid binding. *Hum. Mol. Genet.*, **6**, 311–316.

Saxena,A., Gries,A., Schwarzenbacher,R., Kostner,G.M., Laggner,P. and Prassl,R. (1998) Crystallization and preliminary X-ray crystallographic studies on apolipoprotein H (β2-glycoprotein-I) from human plasma. *Acta Crystallogr. D*, **54**, 1450–1452.

Schousboe,I. (1988) Inositolphospholipid-accelerated activation of prekallikrein by activated factor-XII and its inhibition by β-2-glycoprotein-I. *Eur. J. Biochem.*, **176**, 629–636.

Shi,W., Chong,B.H., Hogg,P.J. and Chesterman,C.N. (1993) Anticardiolipin antibodies block the inhibition by β2-glycoprotein I of the factor Xa generating activity of platelets. *Thromb. Haemost.*, **70**, 342–345.

Steinkasserer,A., Estaller,C., Weiss,E.H., Sim,R.B. and Day,A.J. (1991) Complete nucleotide and deduced amino-acid-sequence of human β-2-glycoprotein-I. *Biochem. J.*, **277**, 387–391.

Terwilliger,T.C. and Berendzen,J. (1999) Automated structure solution of MIR and MAD. *Acta Crystallogr. D*, **55**, 849–861.

Wiles,A.P., Shaw,G., Bright,J., Perczel,A., Campbell,I.D. and Barlow,P.N. (1997) NMR studies of a viral protein that mimics the regulators of complement activation. *J. Mol. Biol.*, **272**, 253–265.

Received August 9, 1999; revised and accepted September 21, 1999